New Methods towards High-Resolution Reconstruction of Saturn's Rings

Dell Li, Maiya Qiu, Mark Zhao
Mentor: Dr. Ryan Maguire

MIT PRIMES October Conference
October 24, 2026

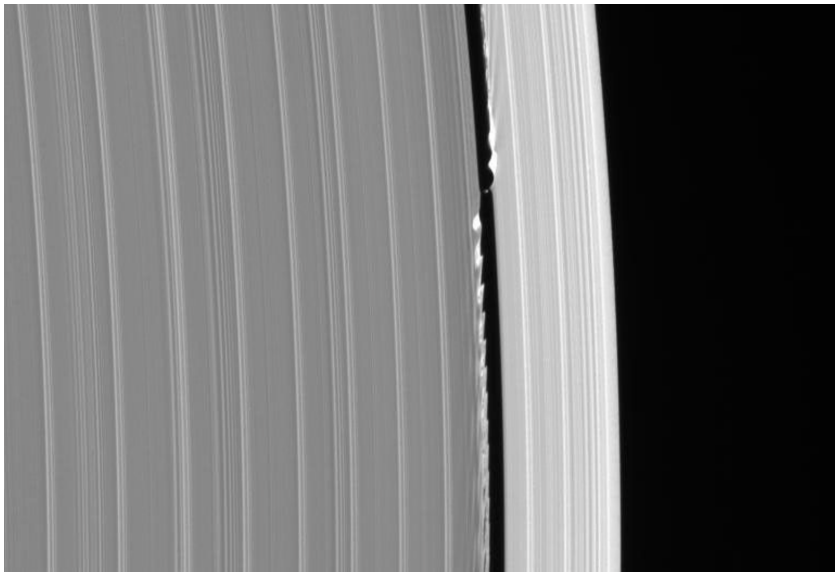
Outline

1. Introduction
2. Background
3. The Bifurcation Problem
4. Root-Finding Methods
5. Local Reliability
6. Concluding Remarks

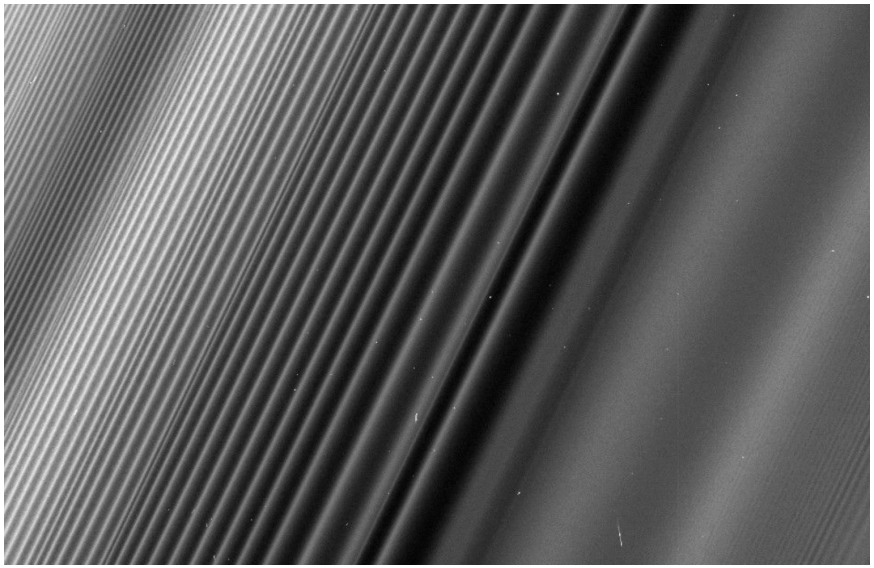
Introduction: Radio Occultation

- Cassini-Huygens mission (2004 – 2017): Radio Science Subsystem (RSS) used to send beams of high-precision radio waves back to Earth.
- Radio signals are diffracted as it passes through Saturn's rings.
- We have the math and physics to invert this process, essentially turning diffracted nonsense into high resolution ring profiles.

Saturn's Rings



(a) Ripples due to Daphnis passing.



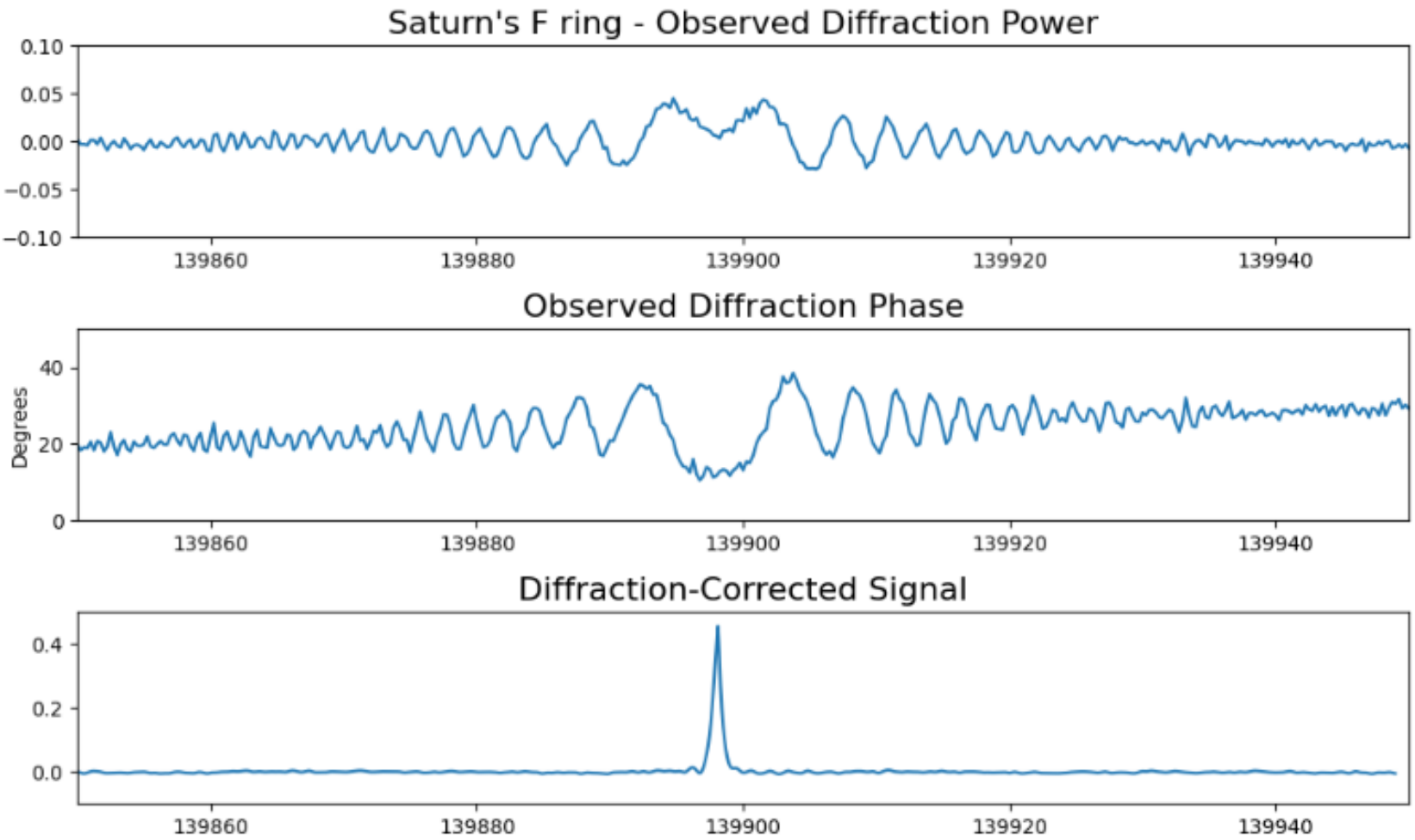
(b) Spiral density waves.

- Note that these are taken in visible light; reconstructed ring profiles using radio signals can resolve much finer detail.

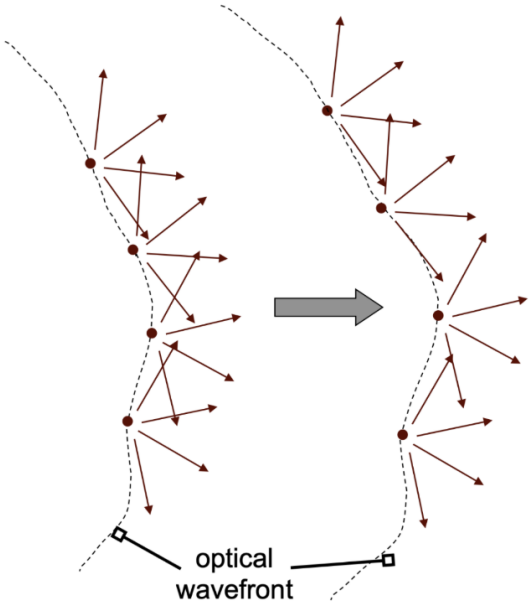
Project Focus

- Complete radio ring profiles: 1 km spatial resolution.
- Previous years' PRIMES: Faster and more accurate 100m resolution profiles for selected Cassini orbits.
- We aim to improve the accuracy whilst maintaining the speed of the reconstructions to achieve the best resolutions (20m, 10m) possible for the instruments used on the RSS.

Example: Reconstructed Radio Signal



Background: Huygens–Fresnel Principle



- Each point on a wavefront acts as a secondary source, emitting a spherical wave.
- The propagated field is the superposition of these waves.
- Depending on their phases, the contributions can reinforce or cancel one another.

The Diffraction Integral

The wave contributions are summed over all (relevantly close) points on the screen.

Reconstruction Formula

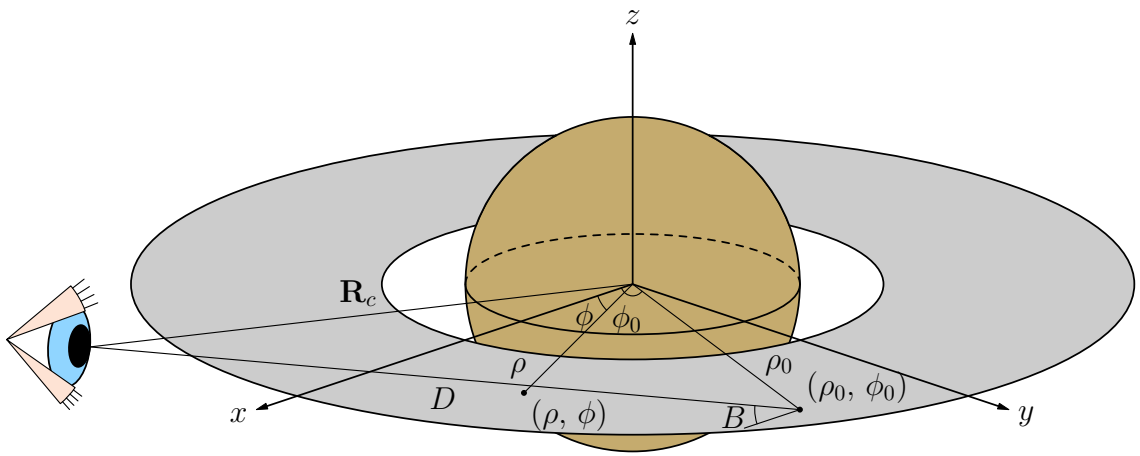


Figure 2: Geometric model of the signal diffraction, parameters labeled.

Letting $\hat{T}$ denote the diffracted complex transmittance,

$$\hat{T}(\rho_0) = \frac{\mu_0}{i\lambda} \int_0^\infty \rho T(\rho) \int_0^{2\pi} \frac{e^{i\psi(\phi_0,\rho_0;\rho,\phi)}}{|R_c - \rho|} d\phi d\rho.$$

- μ_0 is a constant; λ is the wavelength; ψ is the Fresnel phase.

  We want to invert this to produce the original $T(\rho)$.

Stationary Phase Approximation

- The integral with $e^{i\psi(\phi_0;\rho_0;\rho,\phi)}$ is highly oscillatory and can be approximated by the greatest contributions, i.e. stationary phase angles ϕ where $\psi_\phi = 0$.
- In the case of multiple solutions the contributions of each ϕ_s are simply summed.
- Aim: Find these roots numerically as accurately as possible.

Root Bifurcation

- Previous algorithms assumed (and usually was only able to find) a stable global min root.

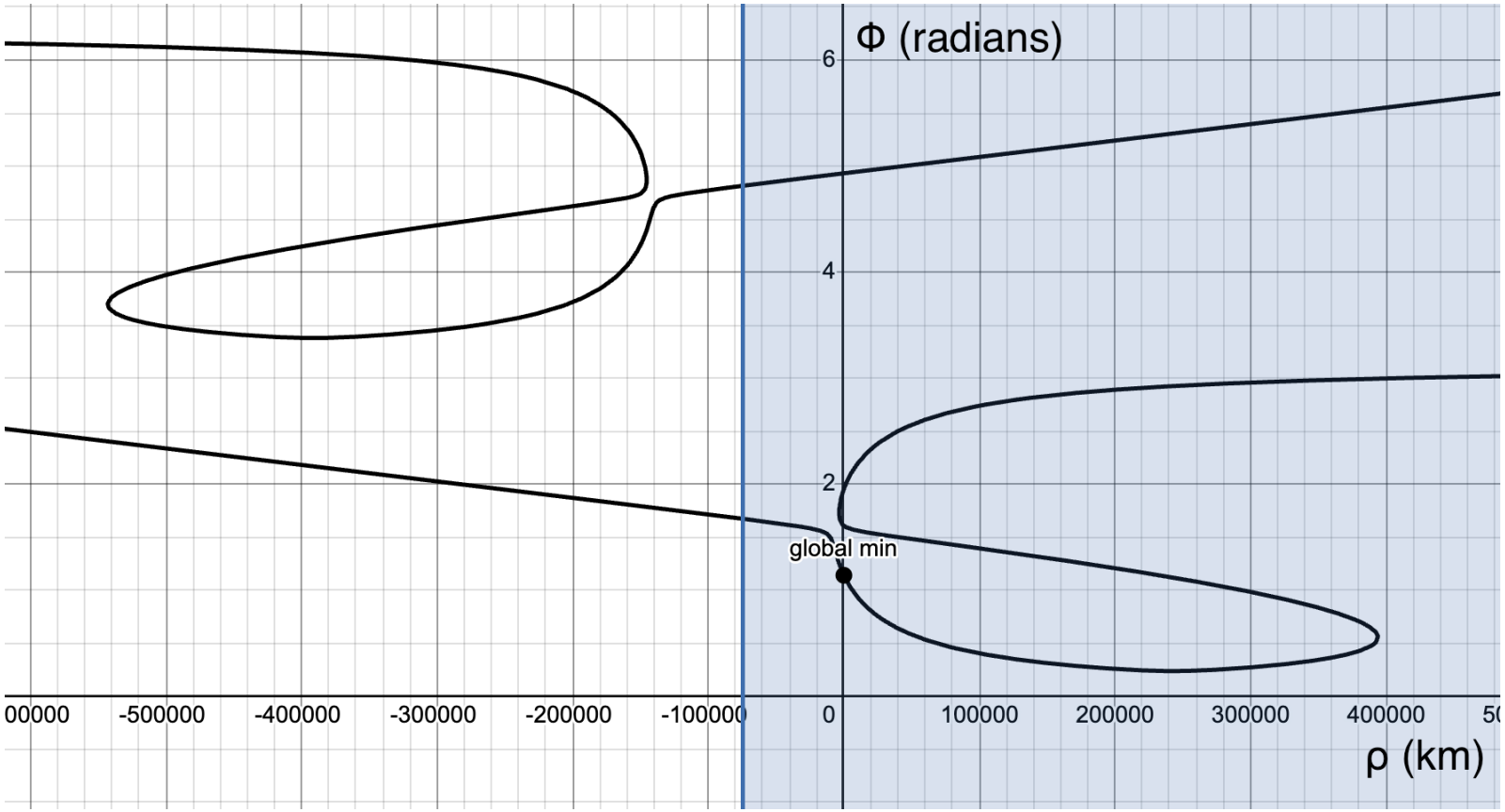


Figure 3: Near Ring C stationary angle solutions.

- Solutions exhibit an *imperfect pitchfork bifurcation*. (Bifurcation point: $\psi_{\phi\phi} = 0$).
- Bottom two roots vanish outside the relevant range of 10k, 20k km.

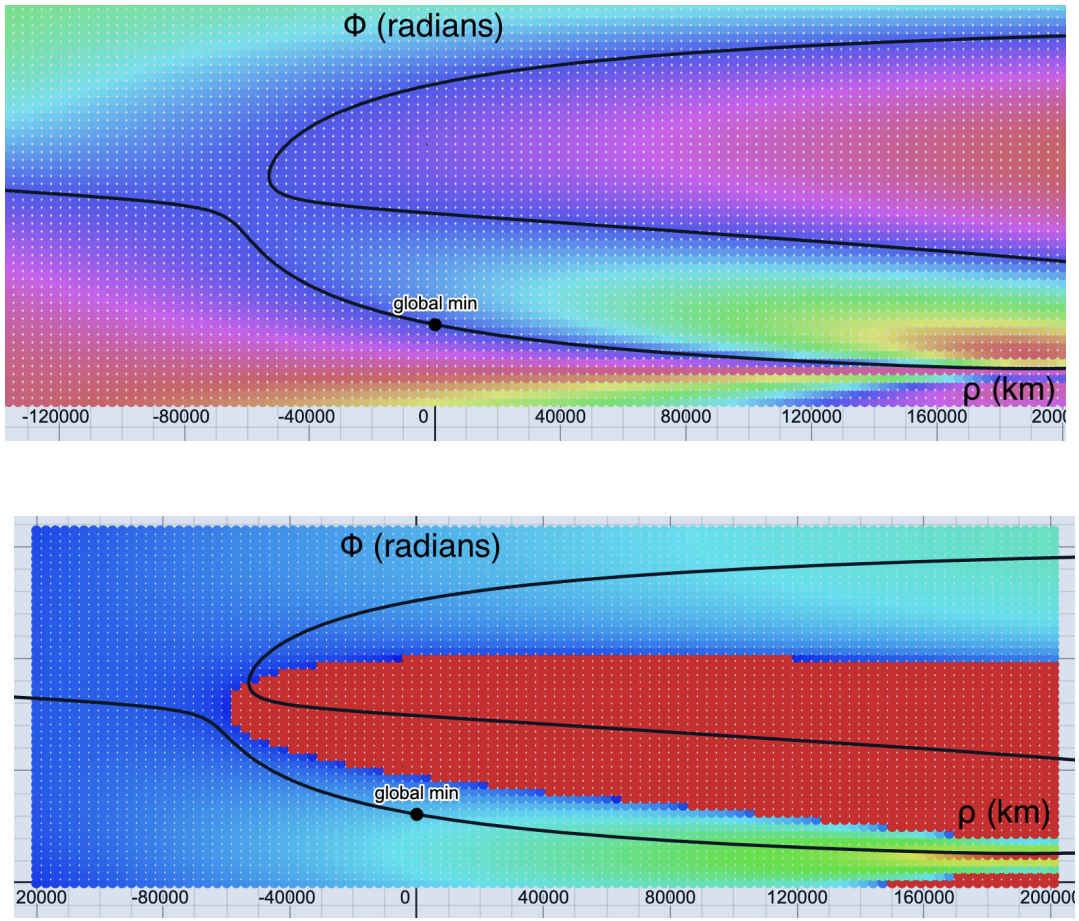


Figure 4: Color map of stationary phase solutions by ψ' (top) and ψ'' (bottom).

Previous root-finding: Halley's Method

- Previous methods (Halley's Method taking the initial guess as ϕ_0) fail to track the unstable root branches.

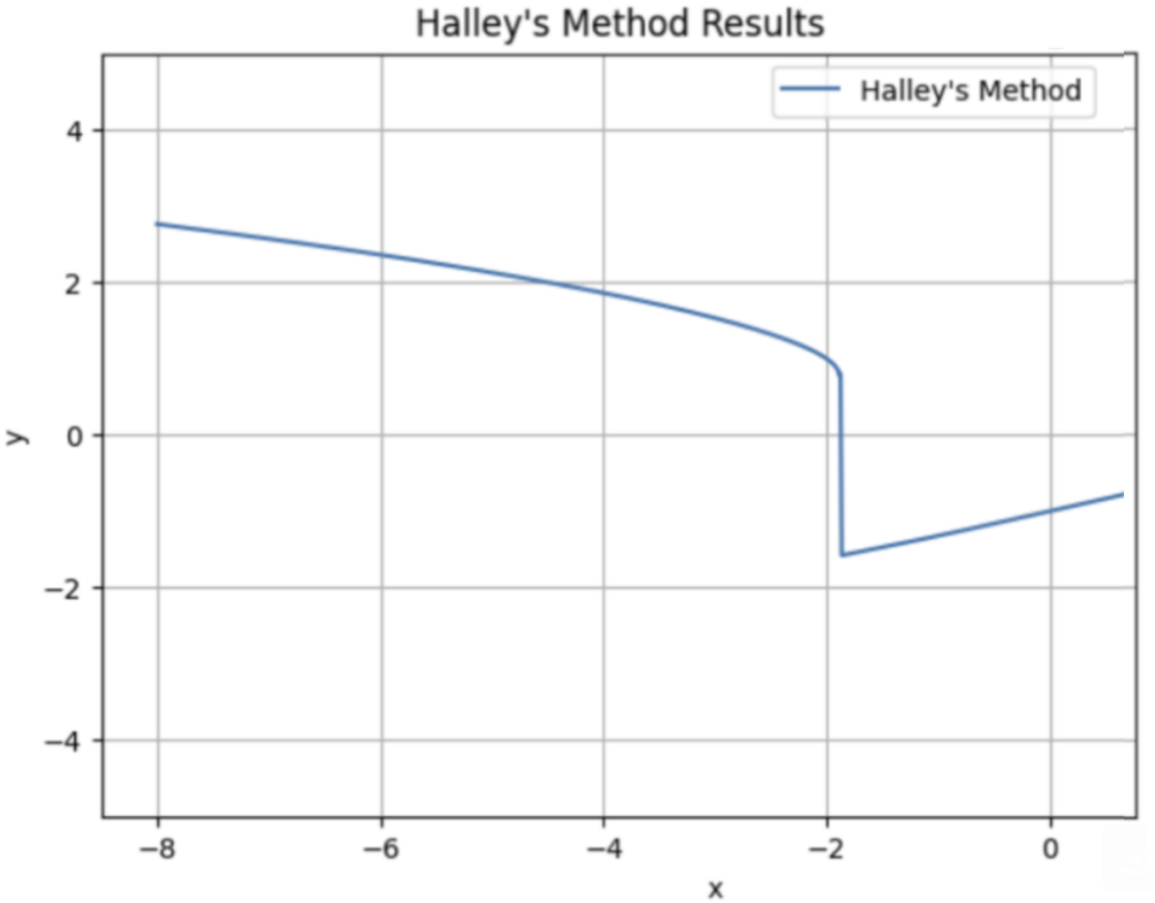


Figure 5: Halley's Method jumping to a different root branch at around $x = -2$.



Figure 6: Basins of attraction (Halley's Method on actual data)

.

Central Question

(Under the context of this phase function), how can we accurately track all three roots without blowing up our computing time?

To give you an idea...

$$\psi(\rho_0, \phi_0; \rho, \phi) = kD[\sqrt{1 + 2\xi + \eta} - (1 + \xi)].$$

$$\begin{cases} \xi = \dfrac{\cos B(\rho_0 \cos\phi_0 - \rho\cos\phi)}{D} \\ \eta = \dfrac{\rho_0^2 + \rho^2 - 2\rho\rho_0\cos(\phi - \phi_0)}{D^2} \\ D = |R_c - \rho_0| \end{cases}$$

- We are finding methods that can find the roots of *the derivative of* ψ with respect to ϕ with high accuracy and stability.
- As the global min root branch is stable we can track it by Halley's Method. The remaining pair can be found by a variety of root-finding methods.

Method 1

A Padé approximant replaces f locally by a rational function

$$R_{m,n}(x) = \frac{P_m(x)}{Q_n(x)} = \frac{\sum_{i=0}^{m} a_i x^i}{1 + \sum_{i=1}^{n} b_i x^i}.$$

Its coefficients are chosen so that

$$f^{(\ell)}(x_0) = R^{(\ell)}_{m,n}(x_0), \qquad \ell = 0, 1, \ldots, m+n.$$

Since we are interested in three root branches, we choose $m = 3$, so that the numerator $P_3(x)$ is cubic. As the global min root is known, the remaining factor is a quadratic which provides the locations for the unstable pair of roots.

Padé Approximation continued

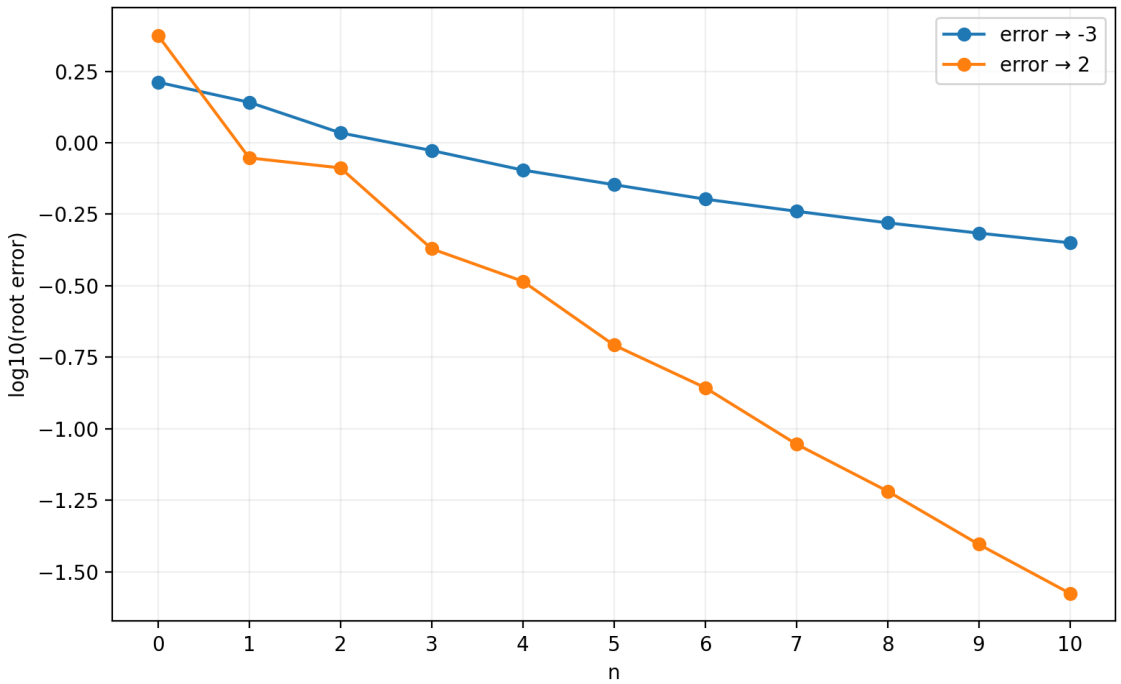


Figure 7: Errors of Padé Approximation with growing denominator degree n

- Increasing the denominator degree improves the root accuracy at slower returns while computational time increases cubically.
- We use a cubic denominator to produce an estimate quickly.

Method 2: Pseudo-Arclength Continuation

- (Essentially) takes the point on the curve closest to an initial guess determined by stepping along the tangent of the previous point.

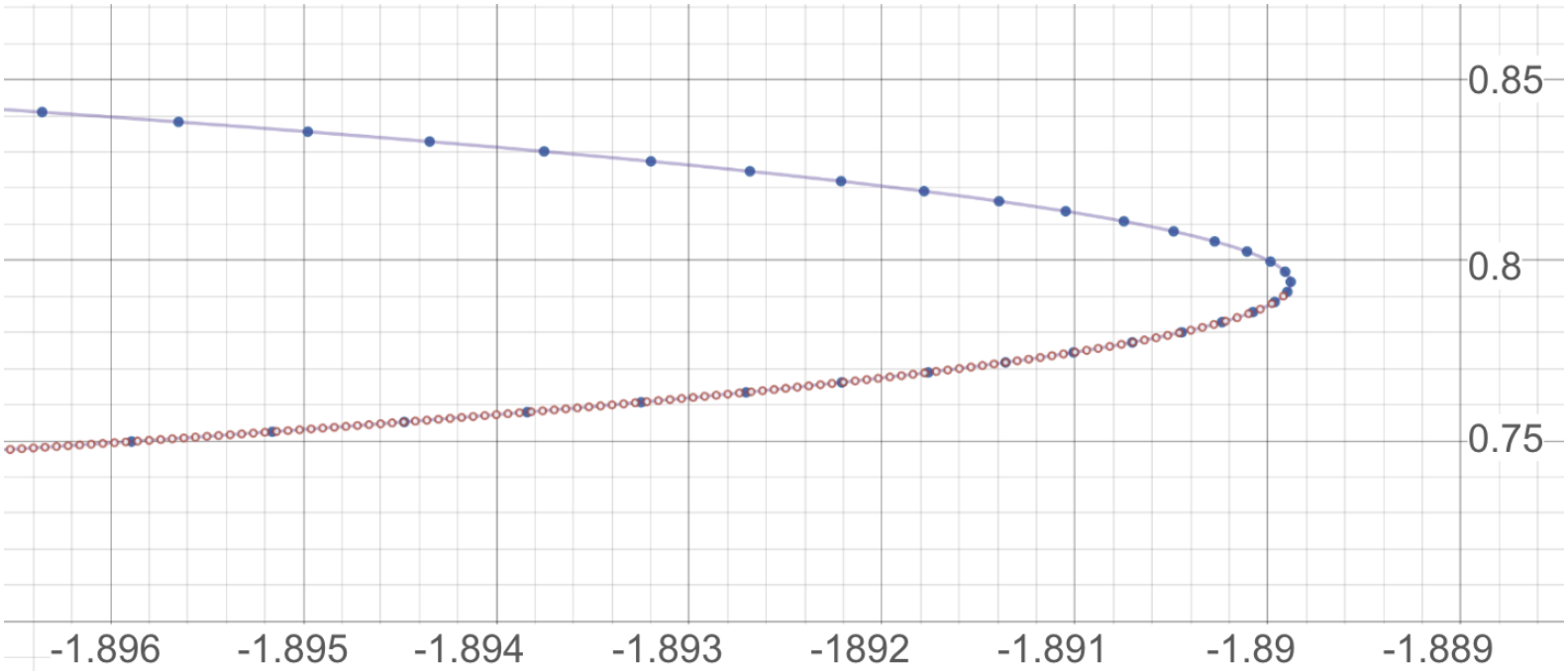


Figure 8: Blue - roots found from PAC; red - points for equidistant ρ interpolated from blue points.

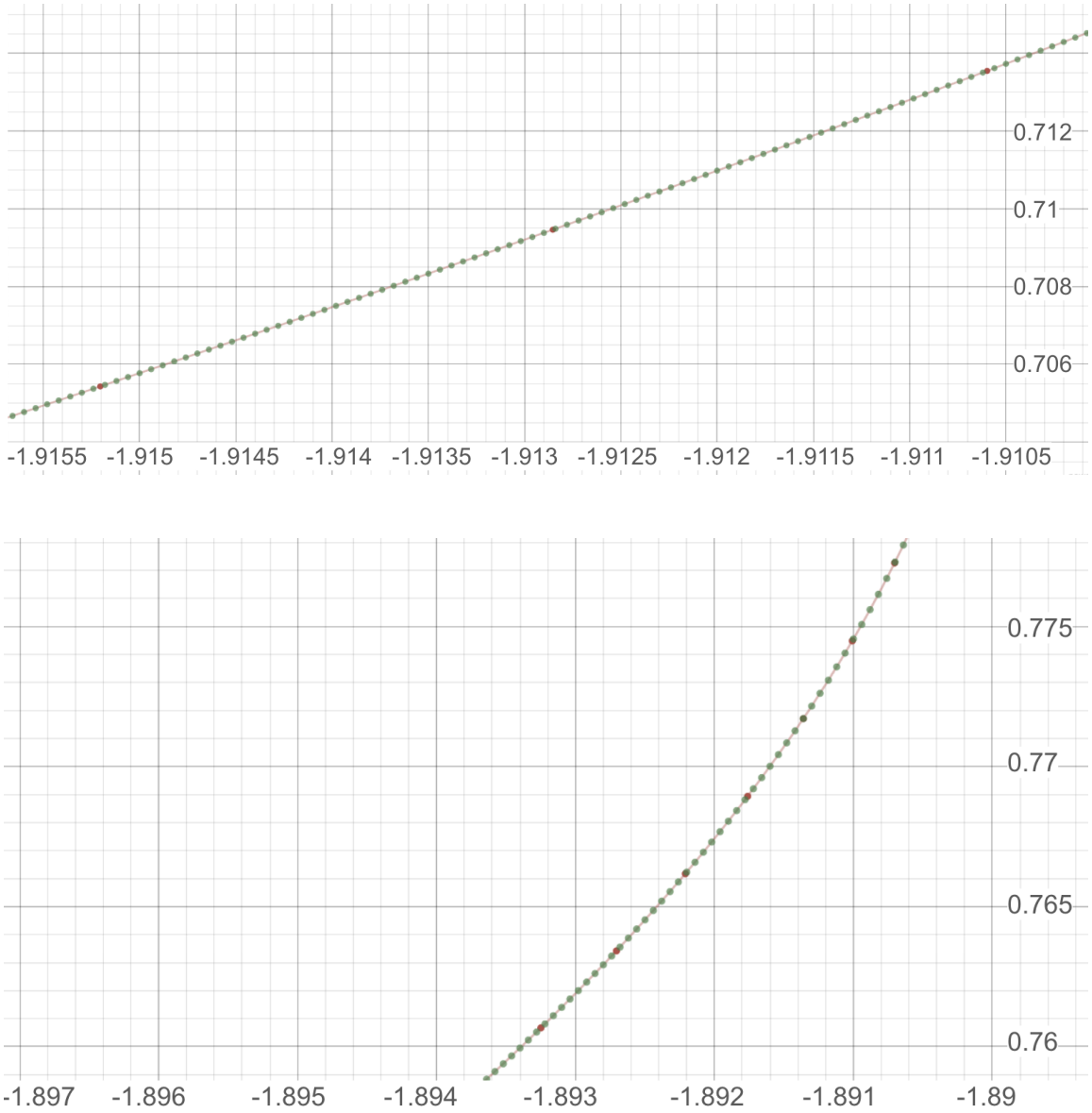
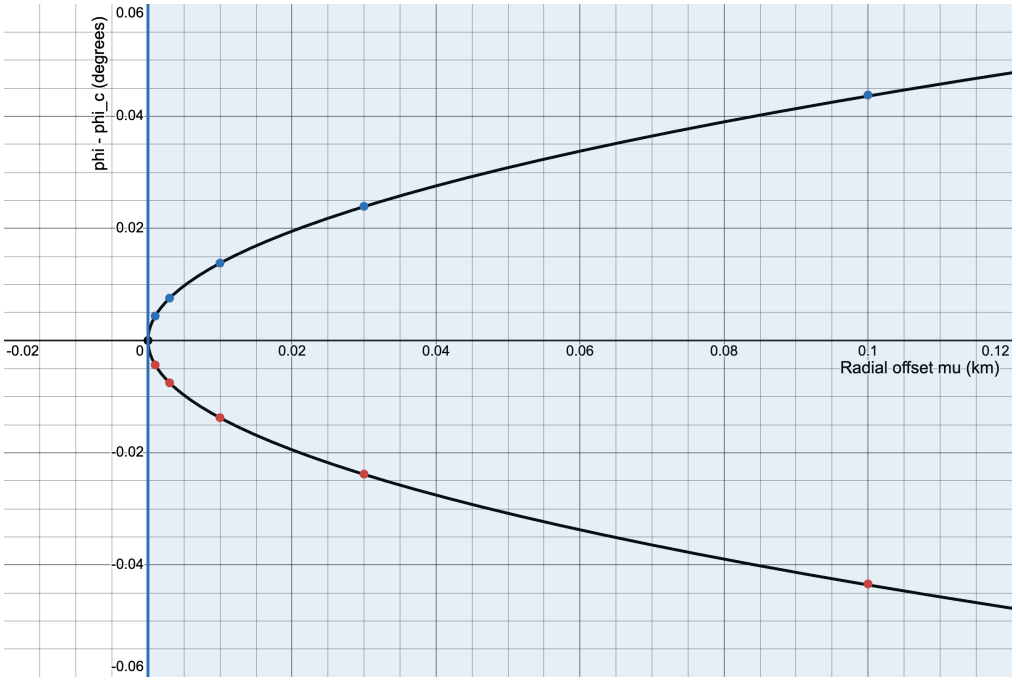


Figure 9: Close-ups of PAC solution finding.

Local Reliability Near a Fold

The previous methods locate Stationary Points. We now check the local integral.



Dots: numerical roots.

Curves: local fold prediction.

Two Stationary Points merge at a **fold**.

Their separation follows the local prediction:

$$d = |\phi_+ - \phi_-| \propto \sqrt{\mu}.$$

$\mu = \rho - \rho_c > 0.$

The phase curvature vanishes at the merger.

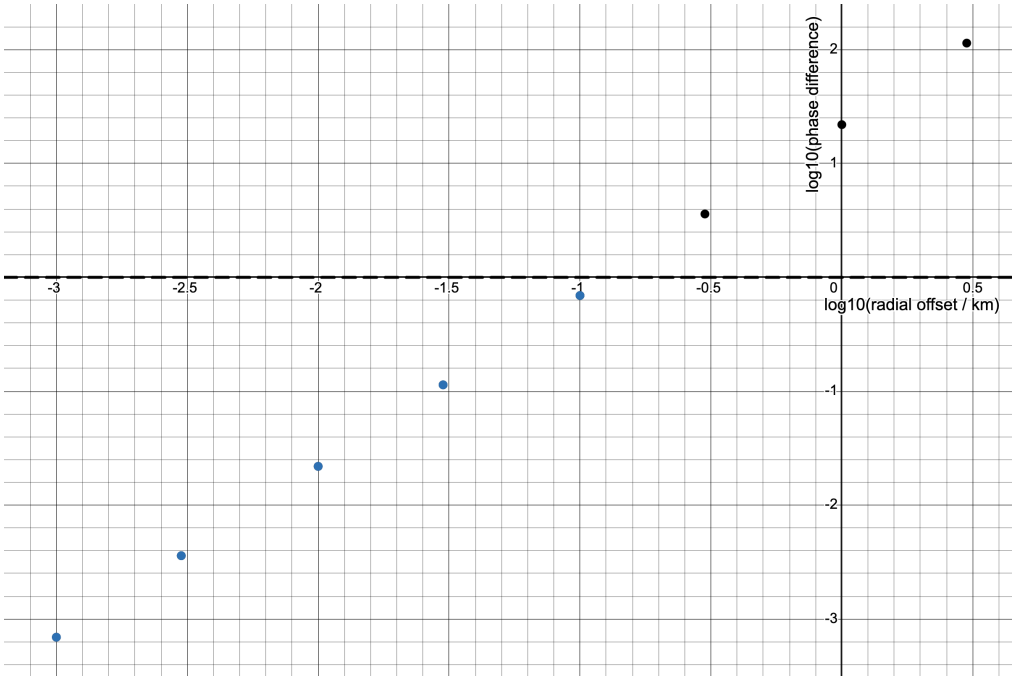
At the fold, the isolated-point approximation is singular.

Model calculation in the stated geometry.

Phase-Based Local Integration

Use the full phase difference between the two Stationary Points:

$$\chi = |\psi(\rho, \phi_+) - \psi(\rho, \phi_-)|.$$



$\chi \leq 1$: **direct integration**
Replace the pair's contribution by integrating its local region.

$\chi > 1$: **retain the approximation**
Use the contributions from isolated Stationary Points.

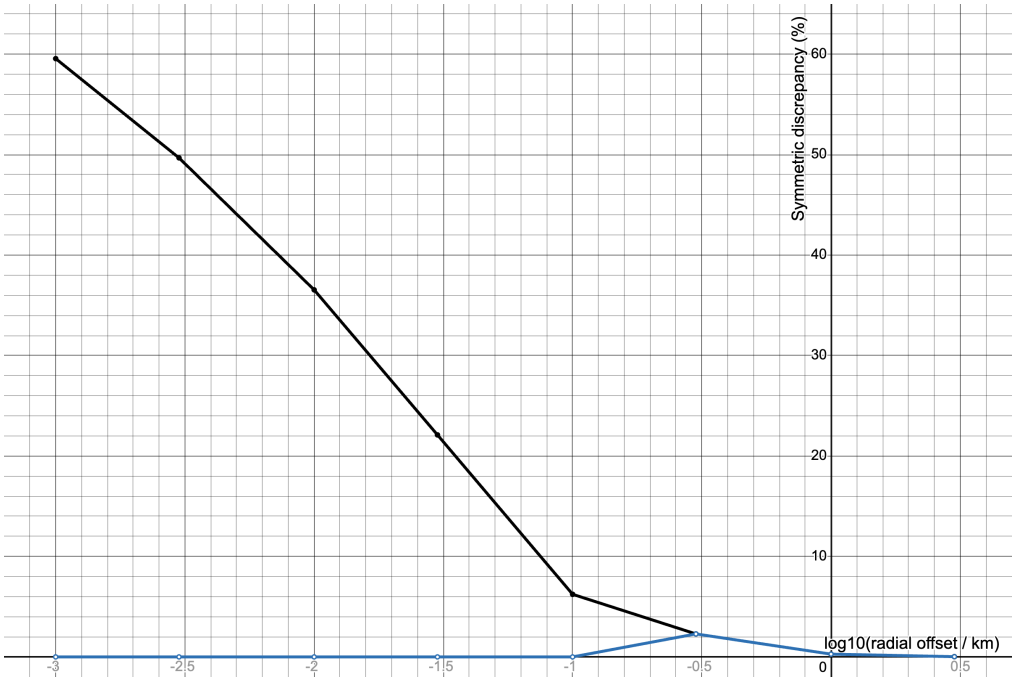
Log–log axes. The line marks $\chi = 1$.

Five of the eight selected offsets use direct integration.

Fixed test threshold. It provides no universal error bound.

Local Comparison at Eight Selected Offsets

Compare the same local angular window, phase and amplitude.



Black: isolated-point approximation.

Blue: selective local integration.

Maximum local discrepancy

Isolated-point method: 59.56%.

Selective integration: 2.29%.

Reference: numerical integration, checked by independent quadrature methods.

$$E_{\mathrm{loc}} = \frac{|I_{\mathrm{loc}}^{\mathrm{method}} - I_{\mathrm{loc}}^{\mathrm{ref}}|}{|I_{\mathrm{loc}}^{\mathrm{method}}| + |I_{\mathrm{loc}}^{\mathrm{ref}}|}.$$

The effect on the complete reconstruction remains unmeasured.

Conclusions

- We found previously unaccounted contributions to the Stationary Points Approximation step of the reconstruction and applied numerical methods to successfully track these bifurcating roots.
- We then tested a phase-based switch to direct integral near a fold, reducing the maximum local symmetric discrepancy.
- (Future) This is an in-progress work with a NASA grant proposal projected to support its eventual implementation for all of Cassini's radio occultation data!

Acknowledgements

We would like to thank our mentor Dr. Ryan Maguire for proposing this project, and his invaluable support and suggestions throughout the program. We would also like to express our heartfelt gratitude to the MIT PRIMES program for making this wonderful opportunity to conduct research possible.

Thank you!